JACS
JOURNAL OF THE AMERICAN CHEMICAL SOCIETY

Communication

pubs.acs.org/JACS

Metabolically Labile Fumarate Esters Impart Kinetic Selectivity to Irreversible Inhibitors

Balyn W. Zaro, Landon R. Whitby, Kenneth M. Lum, and Benjamin F. Cravatt*

The Skaggs Institute for Chemical Biology and Department of Chemical Physiology, 10550 North Torrey Pines Road, La Jolla, California 92037, United States

Supporting Information

ABSTRACT: Electrophilic small molecules are an important class of chemical probes and drugs that produce biological effects by irreversibly modifying proteins. Examples of electrophilic drugs include covalent kinase inhibitors that are used to treat cancer and the multiple sclerosis drug dimethyl fumarate. Optimized covalent drugs typically inactivate their protein targets rapidly in cells, but ensuing time-dependent, off-target protein modification can erode selectivity and diminish the utility of reactive small molecules as chemical probes and therapeutics. Here, we describe an approach to confer kinetic selectivity to electrophilic drugs. We show that an analogue of the covalent Bruton's tyrosine kinase (BTK) inhibitor Ibrutinib bearing a fumarate ester electrophile is vulnerable to enzymatic metabolism on a time-scale that preserves rapid and sustained BTK inhibition, while thwarting more slowly accumulating off-target reactivity in cell and animal models. These findings demonstrate that metabolically labile electrophilic groups can endow covalent drugs with kinetic selectivity to enable perturbation of proteins and biochemical pathways with greater precision.

Covalent small molecules are valuable tools for interrogating biological processes and promising therapeutics for treating human disease.[1] By reacting irreversibly with protein targets, covalent small molecules can produce more complete and sustained pharmacological effects compared to traditional reversible compounds.[1−3] Covalent small molecule−protein adducts also provide a convenient handle for visualizing and quantifying target engagement and selectivity in biological systems.[3−5] Activity-based protein profiling (ABPP) and related chemical proteomic methods have accordingly been utilized to assess the proteome-wide reactivity of electrophilic small molecules, facilitating optimization of on-target activity while minimizing off-target interactions.[3]

Many electrophilic small molecules act by modifying cysteine residues in proteins, and we, and others, have shown that broad-spectrum cysteine-reactive chemical probes can be used to map globally the targets of such electrophilic drugs in native biological systems.[6] Chemical proteomic studies have also revealed that electrophilic drugs often react rapidly with their intended targets in cells, but then show substantial time-dependent increases in proteome-wide reactivity.[4] Minimizing this cross-reactivity, which can confound the interpretation of drug action in biological systems and jeopardize drug safety in humans,[1] presents a major challenge. One potential solution is the use of hyper-electrophilic drugs that bind to proteins in a covalent, reversible manner.[7] Here, we describe an alternative and complementary strategy that achieves kinetic selectivity, where irreversible on-target engagement is preserved and time-dependent proteomic cross-reactivity minimized by endowing covalent small molecules with metabolically labile electrophilic groups.

We recently generated a chemical proteomic map of cysteine residues targeted by the immunomodulatory drug dimethyl fumarate (DMF) in human T cells.[8a] In this study, we found that the hydrolytic product of DMF, monomethyl fumarate, showed negligible reactivity with proteinaceous cysteines. A methyl fumarate-bearing analog of the opioid receptor antagonist naltrexone has also been shown to be thiol-reactive.[8b] We were inspired by these results to consider the fumarate ester as a metabolically labile switch for controlling electrophilic drug activity. In this kinetic selectivity model, treating cells with a fumarate ester drug would produce rapid engagement of the intended drug target(s) on a time scale that outcompetes esterolysis by cellular carboxylesterases (CESs), which would then inactivate excess free drug to prevent slower off-target reactivity (Figure 1A). As a proof-of-concept for achieving kinetic selectivity for irreversible inhibitors, we generated a fumarate ester analogue of the Bruton's tyrosine kinase (BTK) inhibitor Ibrutinib (**1**), which reacts with an active-site cysteine via a terminal acrylamide (Figure 1B).[4,9] Ibrutinib and its fumarate ester analogue (**2**) were further modified with alkyne handles to furnish probes **3** and **4**, respectively.

We confirmed concentration-dependent labeling of BTK by **3** and **4** in Ramos cell lysates using ABPP involving copper-catalyzed azide−alkyne cycloaddition (CuAAC)[10] of probe-labeled proteins to a fluorescent tag followed by SDS-PAGE (Figure S1A).[4] Probe **4** exhibited greater *in vitro* proteomic reactivity than probe **3**, and we also found that **4** reacted more rapidly with cysteine as a model nucleophile (Figure S1B). We next incubated **2** with HEK293T cells expressing human carboxylesterase-1 (hCES1), carboxylesterase-2 (hCES2) or a control protein (methionine aminopeptidase 2, MetAP2; Figure S2A), and found that hCES1-, but not hCES2- or MetAP2-expressing cells converted **2** to the corresponding

Received: October 9, 2016
Published: December 5, 2016

DOI: 10.1021/jacs.6b10589
J. Am. Chem. Soc. 2016, 138, 15841−15844

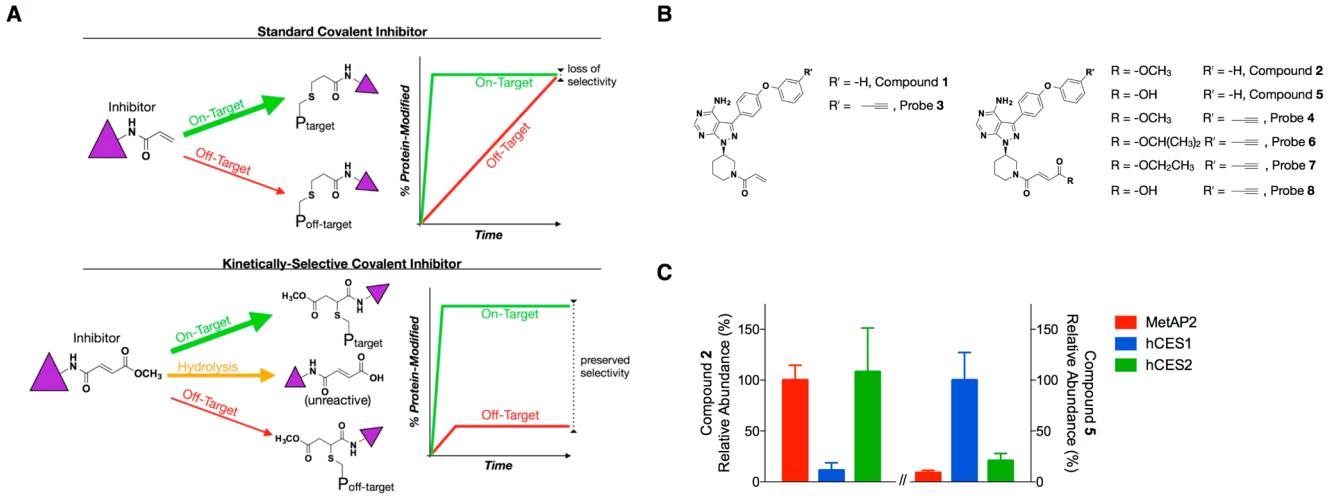

Figure 1. Kinetic selectivity model for covalent small molecules and its application to Ibrutinib. (A) Standard covalent inhibitor (CI). Fast on-target (green arrow) and slower off-target reactivity (red arrow). Kinetically selective CI. Fast on-target (green arrow) and slower off-target reactivity (red arrow), with an intermediary rate of hydrolysis of the electrophilic fumarate ester to unreactive free acid (orange arrow). (B) Ibrutinib-based compounds and probes. (C) **2** is hydrolyzed to inactive **5** by hCES1-, but not hCES2- or control protein (MetAP2)-transfected HEK293T cells. Cells were treated with **2** (10 μM, 1 h) prior to extraction and LC-MS analysis to quantify relative amounts of **2** and **5**.

carboxylic acid (**5**, Figure 1C). In contrast, Ibrutinib (**1**) was unaffected by either CES (Figure S2B).

We had previously found that tumor xenografts express high CES activity originating mainly from stromal/host cells.[11] We attempted to mimic this endogenous environment using a dual-cell culture system, where Ramos cells were cocultured with HEK293T cells stably expressing hCES1 (Figure S3). Using a 6:1 ratio of Ramos and HEK293T cells expressing either hCES1 or MetAP2, we found that hCES1, but not MetAP2, produced a marked reduction in the *in situ* proteome-wide reactivity of **4**, while only modestly reducing the potency (~10-fold) of this probe for BTK (Figure S4). In contrast, hCES1 had no effect on the proteome-wide reactivity of **3**. Time course studies verified these findings, where the initial engagement of BTK by **3** or **4** was followed by substantial proteome-wide reactivity that increased over 24 h, except under conditions where **4** was incubated with Ramos-hCES1-HEK293T cocultures, which instead furnished rapid and sustained labeling of BTK with negligible increases in background proteome cross-reactivity (Figures 2 and S5). These results, taken together, support a model where hCES1 imparts kinetic selectivity to **3**. Notably, the heightened reactivity of **4** compared to **3** seen in our *in vitro* studies (Figure S1) was not observed *in situ*, suggesting that some basal level of fumarate ester metabolism in human cells, independent of exogenous hCES1 expression, may serve to normalize the proteomic reactivity of **3** and **4**.

We next evaluated high-occupancy targets of **1** and **2** by performing competition experiments. Cocultures of Ramos and hCES1- or MetAP2-HEK293T cells were treated with **1** or **2** (1 nM–10 μM, 1 h) followed by treatment with **3** (200 nM, 1 h). Gel-based ABPP revealed complete blockade of BTK by both **1** and **2**, with **1** showing ~10-fold greater potency (Figure S6A,B). The potency of BTK blockade by **2** was only marginally affected in the presence of hCES1 (Figure S6A,B), further supporting that engagement of this kinase occurs at a rate that exceeds CES-mediated metabolism of fumarate ester analogues of **2**. We also performed competition experiments using quantitative mass spectrometry (MS)-based proteomics (ABPP-SILAC (stable isotope labeling with amino acids in cell

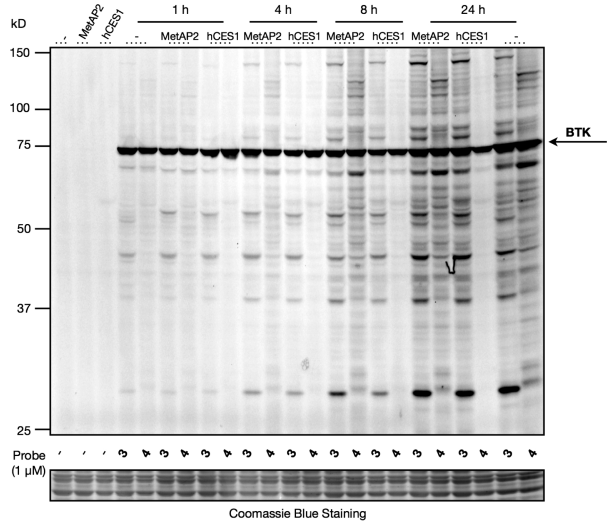

Figure 2. hCES1 suppresses the proteome-wide reactivity of probe **4**. Ramos cells cocultured with HEK293T cells expressing hCES1 or MetAP2, or Ramos only cell culture preparations (–) were treated with **3** or **4** (1 μM, 0–24 h). Gel-based ABPP revealed rapid BTK engagement and time-dependent increases in proteome-wide reactivity for both probes, except for **4** in the presence of CES1, where proteome-wide reactivity was blocked.

culture)[12]), as described previously.[4] Isotopically labeled cocultures of Ramos cells with hCES1- or MetAP2-HEK293T cells were treated with DMSO or inhibitor (**1** or **2** ; 10 μM, 1 h) prior to addition of **3** (1 μM, 1 h). Conjugation of **3**-labeled proteins to an azide-biotin tag, followed by streptavidin enrichment and LC-MS-based proteomics identified high-occupancy targets of **1** that matched those reported previously[4] (Figure S6C and Table S1). None of these targets was affected by hCES1 expression. Inhibitor **2** showed only three high-occupancy targets, two of which (BTK and TEC) were hCES1-insensitive, whereas a third (BLK) showed markedly reduced inhibition by **2** in the presence of hCES1 (Figure S6C). The fewer high-occupancy off-targets for **2** compared to **1** indicates the fumarate reactive group imparts improved selectivity to the

DOI: 10.1021/jacs.6b10589
J. Am. Chem. Soc. 2016, 138, 15841–15844

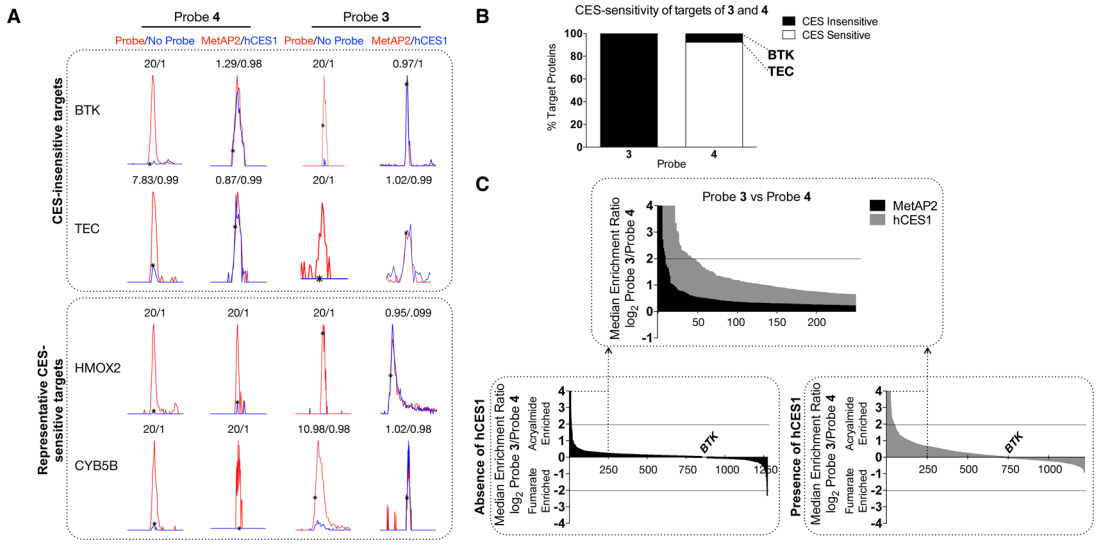

Figure 3. Characterization and hCES1-dependency of targets of **3** and **4**. (A) Representative MS1 spectra for probe targets. Ratios >20 are assigned as 20 values. (B) hCES1-sensitivity of targets of **3** and **4**. Proteins showing ratios of ≥2.5 in MetAP2/hCES1 ABPP-SILAC experiments were assigned as CES-sensitive. (C) Comparison of the reactivity of **3** and **4**. Cocultures of Ramos and HEK293T cells expressing hCES1 or MetAP2 were treated with **3** or **4** (1 μM, 24 h). Average SILAC ratios for proteins from three experiments are shown.

Ibrutinib scaffold (as has been observed for other beta-substitutions to the acrylamide of this inhibitor).[4] The limited number of high-occupancy targets for **1** and **2** further suggested that the substantial concentration- and time-dependent proteome-wide cross-reactivity observed for the corresponding probes **3** and **4** (Figures 2 and S4−S5) likely reflected low-stoichiometry interactions. We set out to identify these proteins and assess the impact of CES expression on their probe reactivity by ABPP-SILAC. We catalogued proteins that reacted with **3** and/or **4** by performing probe (1 μM, 24 h) vs no-probe (DMSO) experiments, which identified ∼30−40 proteins that showed high probe/DMSO ratios (>4) in **3** or **4**-treated cells (Figure 3A and Table S1). The majority of these targets showed greatly reduced reactivity with **4** in cocultures of Ramos with hCES1- versus MetAP2-HEK293T cells (Figure 3A,B). Exceptions were BTK and TEC (another high potency target of Ibrutinib),[9] which reacted with **4** in a CES-insensitive manner (Figure 3A,B and Table S1). In contrast, hCES1 had a negligible effect on the reactivity of targets with **3** (Figure 3A,B and Table S1).

We next directly compared the proteomic reactivities of **3** and **4** (1 μM, 24 h). In control Ramos-MetAP2-HEK293T cocultures, **3** and **4** showed comparable reactivity with a handful of proteins being preferentially labeled by one or the other probe (Figure 3C and Table S1). In contrast, in Ramos-hCES1-HEK293T cocultures, **3** showed much greater proteomic reactivity than **4** (Figure 3C and Table S1), consistent with CES-mediated attenuation of **4** reactivity.

Having established that **4** exhibits kinetic selectivity in cell models expressing hCES1, we wondered whether this concept applied *in vivo*. Rodents express an elaborate network of CES enzymes compared to humans,[13] so we also tested an *O*-isopropyl fumarate analogue of Ibrutinib (**6**) (Figure 1B) to determine if it showed different CES-sensitivity in mice to compared to **4**. Probe **6**, as well as the *O*-ethyl analogue **7** (Figure 1B) reacted similarly with BTK compared to **4** (Figure S7). We treated mice with **3**, **4**, and **6** or vehicle (20 mg/kg) for 2 h and visualized probe-reactive proteins in tissues by gel-based ABPP. All probes reacted with BTK in the spleen, and these labeling events were blocked by pretreatment with **1** (20 mg/kg, 2 h) (Figure 4A). Importantly, **4** and **6** exhibited much

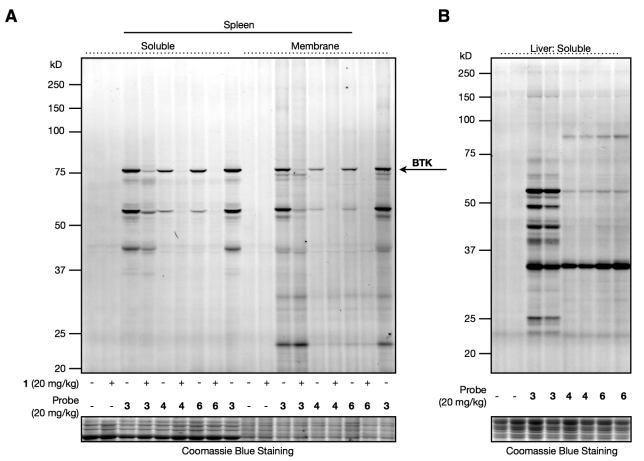

Figure 4. Characterization of probe reactivity *in vivo*. Gel-based ABPP of spleens (A) or livers (B) from mice treated intraperitoneally with probes **3**, **4**, or **6** (20 mg/kg, 2 h). For panel A, animals mice were pretreated with vehicle or Ibrutinib (20 mg/kg, 2 h).

less off-target reactivity compared to **3** in tissue proteomes (Figures 4A,B and S8), indicating that the fumarate ester probes were metabolized by mouse CESs *in vivo*. Also consistent with this conclusion, we found that **4** and **6** were rapidly metabolized in mouse plasma with half-lives of 0.751 and 1.90 min, respectively (Figure S9A), and these half-lives were substantially extended (25.5 and 352 min, respectively) by pretreatment with a CES inhibitor JZL184[15] (10 μM, 1 h) (Figure S9B). In contrast, probe **3** was stable in mouse plasma even in the absence of the CES inhibitor (half-life of 168 min) (Figure S9A). Finally, we should note that, whereas **4** and **6** showed substantial reactivity with BTK *in vivo*, the extent of BTK engagement appeared consistently lower than that of probe **3**, possibly reflecting the reduced potency displayed by fumarate ester analogues of Ibrutinib for BTK or that CES

DOI: 10.1021/jacs.6b10589
J. Am. Chem. Soc. 2016, 138, 15841−15844

metabolism is sufficiently high in mice to compete with full labeling of BTK by these probes.

Our results, taken together, demonstrate that incorporating a fumarate ester electrophile into the Ibrutinib scaffold furnishes an irreversible inhibitor with striking kinetic selectivity for BTK in cell and animal models due to CES-dependent metabolic inactivation. The time scale for CES-mediated hydrolysis of probe **4** appears appropriately positioned to proceed more slowly than probe reactivity with the preferred target BTK, but faster than the proteome-wide cross-reactivity observed for this probe in the absence of hCES1. Importantly, the kinetic selectivity of the fumarate ester probes persisted in cell models over the entire 24 h time-period in the presence of hCES1, which contrasted with the continuous, time-dependent increases in proteome-wide reactivity observed for the acrylamide probe **3**. Considering that covalent inhibitors are often used in pharmacological studies that require one or more days of treatment (e.g., to assess cytotoxicity),[4,14] the ability to impart kinetic selectivity upon probes should improve interpretability of such experiments by minimizing confounding time-dependent off-target reactions. We should note that some protein targets of terminal acrylamides may not accommodate fumarate ester analogues without substantial reductions in potency, and future work will be required to determine the generality and extent to which such reactive groups can be interchanged. It may alternatively be possible to achieve kinetic selectivity with other metabolically vulnerable electrophilic groups such as acrylates and thioacrylates. Additionally, proteins with short half-lives may be less suitable for targeting by kinetic selectivity. Regardless, our data should encourage the consideration of fumarate esters as starting points for the development of covalent inhibitors with potentially improved selectivity profiles in living systems. Indeed, one could speculate that DMF itself exploits the principle of kinetic selectivity to produce immunosuppression with limited side effects in humans.

■ ASSOCIATED CONTENT

Supporting Information

The Supporting Information is available free of charge on the ACS Publications website at DOI: 10.1021/jacs.6b10589.

Protein characterization (XLSX)
Experimental details (PDF)

■ AUTHOR INFORMATION

Corresponding Author

*cravatt@scripps.edu

ORCID

Benjamin F. Cravatt: 0000-0001-5330-3492

Author Contributions

B.W.Z. and B.F.C. designed experiments and interpreted results. B.W.Z. performed experiments and synthesized compounds. L.R.W. provided reagents and synthesized compounds. K.M.L. assisted with proteomics analysis. B.W.Z. and B.F.C. wrote the paper.

Funding

This work was supported by NIH (CA087660, DA033760), American Cancer Society (B.W.Z., PF-15-142-01-CDD), and Pfizer.

Notes

The authors declare no competing financial interest.

■ ACKNOWLEDGMENTS

We thank M. Hayward and A. Gilbert (Pfizer), K. Backus and B. Lanning for helpful discussions, and K. Masuda for technical assistance. We thank M. Cameron (Scripps Florida) for performing plasma stability studies.

■ REFERENCES

(1) (a) Liu, Q.; Sabnis, Y.; Zhao, Z.; Zhang, T.; Buhrlage, S. J.; Jones, L. H.; Gray, N. S. *Chem. Biol.* **2013**, *20*, 146. (b) Mah, R.; Thomas, J. R.; Shafer, C. M. *Bioorg. Med. Chem. Lett.* **2014**, *24*, 33.

(2) Singh, J.; Petter, R. C.; Baillie, T. A.; Whitty, A. *Nat. Rev. Drug Discovery* **2011**, *10*, 307.

(3) Cravatt, B. F.; Wright, A. T.; Kozarich, J. W. *Annu. Rev. Biochem.* **2008**, *77*, 383.

(4) Lanning, B. R.; Whitby, L. R.; Dix, M. M.; Douhan, J.; Gilbert, A. M.; Hett, E. C.; Johnson, T. O.; Joslyn, C.; Kath, J. C.; Niessen, S.; Roberts, L. R.; Schnute, M. E.; Wang, C.; Hulce, J. J.; Wei, B.; Whiteley, L. O.; Hayward, M. M.; Cravatt, B. F. *Nat. Chem. Biol.* **2014**, *10*, 760.

(5) Johnson, D. S.; Weerapana, E.; Cravatt, B. F. *Future Med. Chem.* **2010**, *2*, 949.

(6) (a) Backus, K. M.; Correia, B. E.; Lum, K. M.; Forli, S.; Horning, B. D.; González-Páez, G. E.; Chatterjee, S.; Lanning, B. R.; Teijaro, J. R.; Olson, A. J.; Wolan, D. W.; Cravatt, B. F. *Nature* **2016**, *534*, 570−574. (b) Medina-Cleghorn, D.; Bateman, L. A.; Ford, B.; Heslin, A.; Fisher, K. J.; Dalvie, E. D.; Nomura, D. K. *Chem. Biol.* **2015**, *22*, 1394. (c) Patricelli, M. P.; Janes, M. R.; Li, L. S.; Hansen, R.; Peters, U.; Kessler, L. V.; Chen, Y.; Kucharski, J. M.; Feng, J.; Ely, T.; Chen, J. H.; Firdaus, S. J.; Babbar, A.; Ren, P.; Liu, Y. *Cancer Discovery* **2016**, *6*, 316.

(7) Serafimova, I. M.; Pufall, M. A.; Krishnan, S.; Duda, K.; Cohen, M. S.; Maglathlin, R. L.; McFarland, J. M.; Miller, R. M.; Frodin, M.; Taunton, J. *Nat. Chem. Biol.* **2012**, *8*, 471.

(8) (a) Blewett, M. M.; Xie, J.; Zaro, B. W.; Backus, K. M.; Altman, A.; Teijaro, J. R.; Cravatt, B. F. *Sci. Signaling* **2016**, *9*, rs10. (b) Larson, D. L.; Hua, M.; Takemori, A. E.; Portoghese, P. S. *J. Med. Chem.* **1993**, *36* (23), 3669.

(9) Honigberg, L. A.; Smith, A. M.; Sirisawad, M.; Verner, E.; Loury, D.; Chang, B.; Li, S.; Pan, Z.; Thamm, D. H.; Miller, R. A.; Buggy, J. J. *Proc. Natl. Acad. Sci. U. S. A.* **2010**, *107*, 13075.

(10) Rostovtsev, V. V.; Green, L. G.; Fokin, V. V.; Sharpless, K. B. *Angew. Chem., Int. Ed.* **2002**, *41*, 2596.

(11) Jessani, N.; Humphrey, M.; McDonald, W. H.; Niessen, S.; Masuda, K.; Gangadharan, B.; Yates, J. R.; Mueller, B. M.; Cravatt, B. F. *Proc. Natl. Acad. Sci. U. S. A.* **2004**, *101*, 13756.

(12) Mann, M. *Nat. Rev. Mol. Cell Biol.* **2006**, *7*, 952.

(13) Holmes, R. S.; Wright, M. W.; Laulederkind, S. J. F.; Cox, L. A.; Hosokawa, M.; Imai, T.; Ishibashi, S.; Lehner, R.; Miyazaki, M.; Perkins, E. J.; Potter, P. M.; Redinbo, M. R.; Robert, J.; Satoh, T.; Yamashita, T.; Yan, B.; Yokoi, T.; Zechner, R.; Maltais, L. J. *Mamm. Genome* **2010**, *21*, 427.

(14) (a) Ji, X.; Peng, T.; Zhang, X.; Li, J.; Yang, W.; Tong, L.; Qu, R.; Jiang, H.; Ding, J.; Xie, H.; Liu, H. *Bioorg. Med. Chem.* **2014**, *22*, 2366. (b) Li, X.; Zuo, Y.; Tang, G.; Wang, Y.; Zhou, Y.; Wang, X.; Guo, T.; Xia, M.; Ding, N.; Pan, Z. *J. Med. Chem.* **2014**, *57*, 5112.

(15) (a) Long, J. Z.; Nomura, D. K.; Cravatt, B. F. *Chem. Biol.* **2009**, *16*, 744. (b) Crow, J. A.; Bittles, V.; Borazjani, A.; Potter, P. M.; Ross, M. K. *Biochem. Pharmacol.* **2012**, *84*, 1215.

DOI: 10.1021/jacs.6b10589
J. Am. Chem. Soc. 2016, 138, 15841−15844